

Communication

# Solid-state $^{31}\text{P}$ CP/MAS and static $^{65}\text{Cu}$ NMR characterization of polycrystalline copper(I) dialkyldithiophosphate clusters

Daniela Rusanova<sup>a</sup>, Willis Forsling<sup>a</sup>, Oleg N. Antzutkin<sup>a,\*</sup>, Kevin J. Pike<sup>b,1</sup>, Ray Dupree<sup>b</sup>

<sup>a</sup> Luleå University of Technology, Division of Chemistry, SE 971 87 Luleå, Sweden

<sup>b</sup> University of Warwick, Department of Physics, Coventry CV4 7AL, UK

Received 1 September 2005; revised 20 October 2005

Available online 17 November 2005

## Abstract

Polycrystalline tetra-nuclear  $\text{Cu}_4[\text{S}_2\text{P}(\text{O}-i\text{-C}_3\text{H}_7)_2]_4$ , hexa-nuclear  $\text{Cu}_6[\text{S}_2\text{P}(\text{OC}_2\text{H}_5)_2]_6$ , and octa-nuclear  $\text{Cu}_8[\text{S}_2\text{P}(\text{O}-i\text{-C}_4\text{H}_9)_2]_8(\text{S})$  complexes were synthesized and analyzed by means of solid-state  $^{31}\text{P}$  CP/MAS and  $^{65}\text{Cu}$  static NMR spectroscopy. The symmetries of the electronic environments around each P-site were estimated from the  $^{31}\text{P}$  chemical shift anisotropy (CSA) parameters,  $A_{\text{aniso}}$  and  $\eta$ . The  $^{65}\text{Cu}$  chemical shift and quadrupolar splitting parameters obtained from the experimental  $^{65}\text{Cu}$  NMR spectra of the polycrystalline  $\text{Cu}^{\text{I}}$ -complexes are presented. A solid-state NMR approach for the elucidation of the stereochemistry of poly-nuclear Cu(I) dithiophosphate complexes, when the structural analysis of the systems by single-crystal X-ray diffraction is not readily available, is proposed. © 2005 Elsevier Inc. All rights reserved.

**Keywords:**  $^{31}\text{P}$  CP/MAS NMR; Solid-state  $^{65}\text{Cu}$  NMR; Copper(I); Dialkyldithiophosphate

## 1. Introduction

There is a continuing interest in the structure of  $\text{Cu}^{\text{I}}\text{-S}$ -clusters with sulfide bridges because of their photo-physical properties [1], possible use as models for enzyme-active sites [2], and in relation to the froth flotation of copper containing ores [3]. Copper(I) dialkyldithiophosphate ( $\text{Cu}^{\text{I}}\text{R}_2\text{dtp}$ , R = alkyl) complexes are tetra- [4], hexa- [5] or octa-nuclear [5–7] and contain only ligands of the bridging type. Trimetallic triconnective and tetrametallic tetra-connective coordination patterns of dithiophosphate ligands are observed where the copper atoms reside in trigonal planar sites formed by the sulfur atoms. In the cases of cubane complex all eight copper atoms are also loosely bounded to a S atom in the center of the copper core,  $\text{CuS}_3 \cdots \text{S}$  [8]. The crystallographic data for these clusters

are limited and after the first structural data reported in 1972 [4] about 20 years passed before the single-crystal structure of another  $\text{Cu}(\text{I})\text{-dtp}$  compound was obtained [6].

In this Communication, we present data from solid-state  $^{31}\text{P}$  CP/MAS and static  $^{65}\text{Cu}$  NMR experiments, combined in order to reveal the coordination chemistry of the polycrystalline  $\text{Cu}(\text{I})$  dialkyldithiophosphate complexes. We show how a solid-state NMR approach can be used to elucidate the stereochemistry of these  $\text{Cu}(\text{I})$  compounds, when the structural analysis of the systems by single-crystal X-ray diffraction is not readily available, and how the  $^{65}\text{Cu}$  quadrupolar interaction can be helpful in distinguishing different structural units in these copper(I) systems since different Cu-core structures result in different quadrupolar parameters.

## 2. Results and discussion

### 2.1. $^{31}\text{P}$ CP/MAS NMR data

The  $^{31}\text{P}$  CP/MAS NMR spectra of polycrystalline tetra-nuclear  $\text{Cu}_4[\text{S}_2\text{P}(\text{O}-i\text{-C}_3\text{H}_7)_2]_4$ , **I**, hexa-nuclear  $\text{Cu}_6[\text{S}_2\text{P}(\text{OC}_2\text{H}_5)_2]_6$ , **II**, and octa-nuclear  $\text{Cu}_8[\text{S}_2\text{P}(\text{O}-i\text{-C}_4\text{H}_9)_2]_8(\text{S})$ , **III**, are shown in Fig. 1. The spectra show a complex pattern of peaks, which is characteristic of the polycrystalline nature of the samples.

\* Corresponding author. Fax: +46 920 49 1199.

E-mail address: [Oleg.Antzutkin@ltu.se](mailto:Oleg.Antzutkin@ltu.se) (O.N. Antzutkin).

<sup>1</sup> Current address: ANSTO NMR Facility, c/o Materials and Engineering Science, Lucas Heights Research Laboratories, Private Mail Bag 1, Menai, NSW 2234, Australia.

$\text{H}_5)_2]_6$ , **II**, and octa-nuclear  $\text{Cu}_8[\text{S}_2\text{P}(\text{O}-i\text{-C}_4\text{H}_9)_2]_6(\text{S})$ , **III**, are shown in Fig. 1. The tetra-nuclear complex **I** displays four  $^{31}\text{P}$  resonance lines with 1:1:1:1 relative intensity (Fig. 1A) that reveals a complete structural non-equivalence of the P sites in the cluster, which is in accord with the crystallographic data for the cluster [4]. The symmetry of the electronic environments around each P-site can be estimated from the  $^{31}\text{P}$  chemical shift anisotropy (CSA) parameters,  $\Delta_{\text{aniso}}$  and  $\eta$ , using the definitions:  $\Delta_{\text{aniso}} = \delta_{zz} - \delta_{\text{iso}}$ ;  $\delta_{\text{iso}} = (\delta_{xx} + \delta_{yy} + \delta_{zz})/3$ , where  $\delta_{xx}$ ,  $\delta_{yy}$ , and  $\delta_{zz}$  are the principal values of the chemical shift tensor,  $|\delta_{zz} - \delta_{\text{iso}}| \geq |\delta_{xx} - \delta_{\text{iso}}| \geq |\delta_{yy} - \delta_{\text{iso}}|$  and  $\eta = (\delta_{yy} - \delta_{xx})/\Delta_{\text{aniso}}$  is the asymmetry parameter. The results of simulations of  $^{31}\text{P}$  CSA in the  $^{31}\text{P}$  CP/MAS NMR spectra of  $\text{Cu}_4[\text{S}_2\text{P}(\text{O}-i\text{-C}_3\text{H}_7)_2]_4$  and the other clusters studied here are shown in Table 1. Similar values of  $\Delta_{\text{aniso}}$  with a negative sign for all four non-equivalent phosphorus sites reflect large S–P–S bond angles and the bridging mode of the dialkyldithiophosphate ligands in these clusters in accord with our previous report for binuclear and tetranuclear Zn(II) dialkyldithiophosphate complexes [9].

The  $^{31}\text{P}$  CP/MAS spectrum of **II** is shown in Fig. 1B. A single resonance line at 101.0 ppm with a small shoulder at 99.0 ppm is observed. This suggests that all six dithiophosphate ligands are chemically equivalent. The  $\text{PO}_2\text{S}_2^-$  tetrahedra in all six ligands are not significantly distorted by the steric effects of the short ethyl hydrocarbon tails. According to the reported single-crystal structure of  $\text{Cu}_6[\text{S}_2\text{P}(\text{OC}_2\text{H}_5)_2]_6$ , values of P–S and P–O bond lengths vary only within  $\pm 0.001 \text{ \AA}$  for the six phosphorus atoms and S–P–S and O–P–O bond angles remain the same for all six ligands,

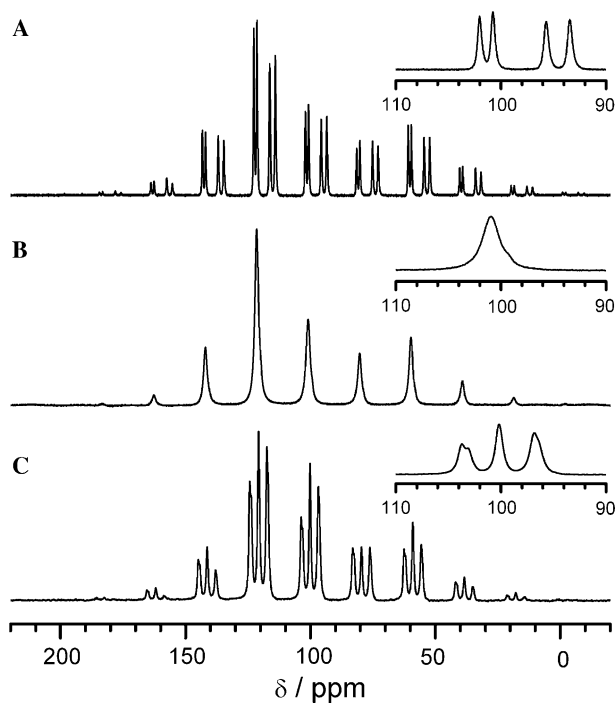


Fig. 1.  $^{31}\text{P}$  CP/MAS NMR spectra at 8.46 T of polycrystalline  $\text{Cu}_4[\text{S}_2\text{P}(\text{O}-i\text{-C}_3\text{H}_7)_2]_4$  (A),  $\text{Cu}_6[\text{S}_2\text{P}(\text{OC}_2\text{H}_5)_2]_6$  (B), and  $\text{Cu}_8[\text{S}_2\text{P}(\text{O}-i\text{-C}_4\text{H}_9)_2]_6(\text{S})$  (C). Thirty-two signal transients. Spinning frequency 3 kHz. Center-bands are shown in the insets.

Table 1  
 $^{31}\text{P}$  chemical shift and chemical shift anisotropy data for the copper(I) dithiophosphate compounds (68.3% confidence interval)

Compound	$\delta_{\text{iso}}$ (ppm)	$\Delta_{\text{aniso}}$ (ppm)	$\eta$	Reference
<b>I</b>	$102.1 \pm 0.1$	$-77.3 \pm 1.2$	$0.28 \pm 0.06$	This work
	$100.8 \pm 0.1$	$-75.2 \pm 1.1$	$0.32 \pm 0.05$	
	$95.7 \pm 0.1$	$-77.5 \pm 0.7$	$0.53 \pm 0.02$	
	$93.5 \pm 0.1$	$-75.0 \pm 0.6$	$0.40 \pm 0.02$	
<b>II</b>	$101.1 \pm 0.1$	$-74.1 \pm 1.0$	$0.28 \pm 0.06$	[13]
<b>III</b>	$103.7 (103.1) \pm 0.1$	$-70.2 \pm 1.2$	$0.50 \pm 0.04$	This work
	$100.2 \pm 0.1$	$-69.1 \pm 1.2$	$0.2 \pm 0.1$	
	$96.8 (96.4) \pm 0.1$	$-64.5 \pm 0.8$	$0.1 \pm 0.1$	

although the O–P–S angles are different and this could be the reason for the observed shoulder [5]. Thus, the chemical equivalence of all P-sites is expected, which in turn gives rise to a single resonance line in the solid-state  $^{31}\text{P}$  NMR spectrum of this complex (see Fig. 1B).

The  $^{31}\text{P}$  CP/MAS NMR spectrum of **III** (Fig. 1C) shows three resonance lines (1:1:1) with a slight sub-splitting of the outer ones (see the inset): the six phosphorus sites in the  $\text{Cu}_8[\text{S}_2\text{P}(\text{O}-i\text{-C}_4\text{H}_9)_2]_6(\text{S})$  are chemically almost equivalent in pairs. This correlates well with the known single-crystal structure of another analogous cubane cluster,  $\text{Cu}_8[\text{S}_2\text{P}(\text{O}-i\text{-C}_3\text{H}_7)_2]_6(\text{S}) \cdot \text{CH}_2\text{Cl}_2$  [5], which has three crystallographically different P sites and it can be expected that the chemically similar polycrystalline cubane compounds with bulky alkyl groups ( $\text{R} = -i\text{-C}_3\text{H}_7$  and  $-i\text{-C}_4\text{H}_9$ ) would have similar  $^{31}\text{P}$  NMR spectra.

## 2.2. Static $^{65}\text{Cu}$ NMR data

The chemical environment of the copper sites in the polycrystalline copper(I) dithiophosphate systems was studied by means of static  $^{65}\text{Cu}$  NMR spectroscopy. Despite the higher natural abundance of the  $^{63}\text{Cu}$  isotope,  $^{65}\text{Cu}$  was preferred in this study since its Larmor frequency falls in a spectral window free from other isotopes and the effect of the quadrupole interaction is slightly smaller. The spectra of the central transitions ( $1/2 \leftrightarrow -1/2$ ) of the studied systems along with simulations are shown in Fig. 2.

It was found that a conventional experiment with strong excitation pulses at a fixed carrier frequency could not excite the whole  $^{65}\text{Cu}$  central-transition range for the NMR spectra of copper(I) dialkyldithiophosphate compounds. Therefore, the complete central-transition spectrum for all of the Cu sites was obtained by stepping the carrier frequency from  $-1.5$  to  $+1.5$  MHz through the CuCl reference frequency [10]. The lineshape observed in the  $^{65}\text{Cu}$  spectrum of **I** is characteristic of a second-order quadrupolar-perturbed central transition and extends over 2 MHz (Fig. 2A). The size of the quadrupolar interaction ( $C_Q = e^2 Qq/h$ ) experienced by a Cu nucleus is characteristic of the molecular environment ( $eQ$  is the nuclear quadrupole moment and  $eq$  is the maximum component of the electric field gradient (EFG) at the nuclear site, and the asymmetry parameter,  $\eta_Q$ , shows the deviation of the

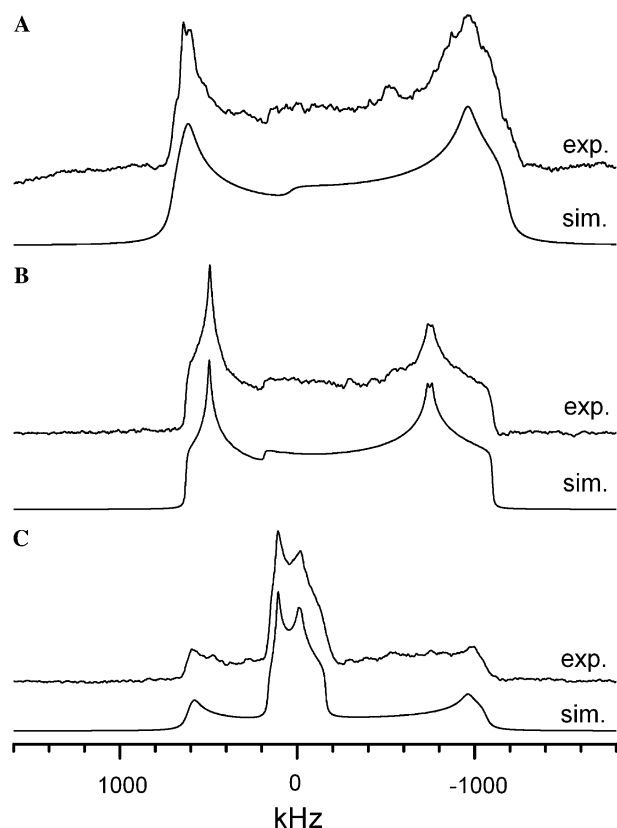


Fig. 2. Static  $^{65}\text{Cu}$  NMR spectra at 14.1 T of polycrystalline  $\text{Cu}_4[\text{S}_2\text{P}(\text{O}-i\text{-C}_3\text{H}_7)_2]_4$  (A),  $\text{Cu}_6[\text{S}_2\text{P}(\text{OC}_2\text{H}_5)_2]_6$  (B), and  $\text{Cu}_8[\text{S}_2\text{P}(\text{O}-i\text{-C}_4\text{H}_9)_2]_6(\text{S})$  (C) along with simulations.

EFG from the axial symmetry,  $0 \leq \eta_Q \leq 1$ ). The complex is expected to contain four structurally non-equivalent Cu sites in planar arrangements of the  $\text{CuS}_3$ -type [4] but the solid-state  $^{65}\text{Cu}$  NMR only reveals a quadrupolar lineshape typical for  $\text{MX}_3$ -sites (M = metal). For these sites a large quadrupolar interaction dominates over both the chemical shift and the dipole–dipole interactions (see Table 2) [11]. A closer look at the lineshape, however, shows that this line could be a superposition of several lines: the left-horn side appears to be slightly split and the right-horn side would be better represented by two or more slightly displaced lines rather than one with a significant quadrupolar interaction.

The  $^{65}\text{Cu}$  NMR spectrum of **II** (Fig. 2B) is similar, but narrower (1.3 MHz), to that of **I**. The differences in  $C_Q$ ,  $\eta_Q$ , and isotropic chemical shifts (see Table 2) indicate the sensitivity of the  $^{65}\text{Cu}$  parameters to the changes in the chemical environment around the Cu sites: a tri-connective

coordination pattern of the ligand is present in both cases with the Cu atoms being in the trigonal planar sites formed by the sulfur atoms. The Cu–S bond length differences are within 0.03–0.04 Å for both compounds, but bond angle variation is much less in the case of **II** (see Table 1 in Appendix A). It is interesting that the resonance pattern of **II** ( $\delta_{\text{iso}} = 300$  ppm) seems to be additionally perturbed by a considerable  $^{65}\text{Cu}$  CSA contribution ( $\Delta_{\text{CS}} = 750$  ppm). According to the reported single-crystal X-ray diffraction structure of  $\text{Cu}_6[\text{S}_2\text{P}(\text{OC}_2\text{H}_5)_2]_6$ , values of Cu–S distance are the same within  $\pm 0.001$  Å for the six copper atoms and S–Cu–S planar bond angles are 118.36°, 116.53°, and 124.06°, for all six atoms [5]. Thus, similar chemical environments for all  $\text{CuS}_3$ -sites were expected that in turn give rise to rather similar resonance lineshapes in the solid-state  $^{65}\text{Cu}$  NMR spectrum. Indeed, sufficient details of the second-order quadrupolar lineshape are seen in the spectrum (Fig. 2B) in spite of the expected overlap of the six  $^{65}\text{Cu}$  resonance patterns. Therefore, the spectrum can be considered as a superposition of the central transitions of the six Cu sites ( $\text{CuS}_3$ ). A single static quadrupolar lineshape alone does not adequately simulate the experimental pattern and a significant  $^{65}\text{Cu}$  CSA contribution is needed to simulate the lineshape.

The static  $^{65}\text{Cu}$  NMR spectrum of the polycrystalline complex, **III**, is shown in Fig. 2C. Two distinguishable quadrupolar lineshapes with relative intensities 1:1 are observed. Large differences in both  $C_Q$  and  $\eta_Q$  for the two resonances reflect the effect of the electronegativity of the closest surroundings (sulfur atoms in all cases) on the Cu-sites and the differing asymmetries of the electric field gradients at Cu atoms in the complex [12]. The whole set of parameters used to simulate the central-transition region of the  $^{65}\text{Cu}$  NMR spectrum of **III** is shown in Table 2. The two lineshapes indicate the presence of two different Cu–S environments: an environment with a higher symmetry is characterized by the lineshape with the smaller  $C_Q$ ; for these sites ( $C_Q = 18.8$  MHz,  $\delta_{\text{iso}} = 400$  ppm) a single static quadrupolar lineshape does not adequately model the experiment and it is necessary to include  $^{65}\text{Cu}$  CSA in the simulations. The sites with the larger quadrupolar constants ( $C_Q = 46.0$  MHz,  $\delta_{\text{iso}} = 120$  ppm) can be considered as a superposition of other copper sites in the copper core, having environments with a lower symmetry. The two quadrupolar lineshapes are substantially overlapped since isotropic chemical shift differences are much smaller, as expected, than the quadrupolar linewidths.

Table 2  
NMR parameters used to simulate the  $^{65}\text{Cu}$  NMR spectra of copper(I) dithiophosphate clusters

Compound	$\delta_{\text{iso}}$ (ppm) $\pm 50$	$C_Q$ (MHz) $\pm 0.2$	$\eta_Q \pm 0.02$	$\Delta_{\text{CS}}$ (ppm) $\pm 50$	$\eta_{\text{CS}} \pm 0.02$	$\chi$ ( $^\circ$ ) $\pm 1$	Reference
<b>I</b>	210	47.6	0.10	0	0.00	0	This work
<b>II</b>	300	45.6	0.17	750	0.00	4	[13]
<b>III</b>	400	18.8	0.41	350	0.00	5	This work
	120	46.0	0.05	0	0.00	0	

The similarity in the quadrupolar coupling constants estimated from the simulations of  $^{65}\text{Cu}$  NMR spectra of **II** and the second site in **III** ( $C_Q = 45.6$  and  $46.0$  MHz, respectively) suggests that the copper sites in **III** with the larger quadrupolar constants are likely to be the sites with chemical environments that are similar to those of the copper sites in **II**, or in other words the copper sites are likely to reside in planar arrangements with the sulfur atoms ( $\text{CuS}_3$ ).

In the analogous cubane copper(I) cluster,  $\text{Cu}_8[\text{S}_2\text{P}(\text{O}-i\text{-C}_3\text{H}_7)_2]_6(\text{S}) \cdot \text{CH}_2\text{Cl}_2$ , the presence of four crystallographically non-equivalent copper sites has been reported [5]. The Cu–S bond lengths for two of them differ within  $0.003 \text{ \AA}$  and for the other two the differences are in the range  $0.005$ – $0.009 \text{ \AA}$ . The S–Cu–S bond angles for the copper sites are all in the range of  $118^\circ$ – $121^\circ$  (see Table S1 in Appendix A). Even though more than two crystallographically different copper sites have been reported, it is reasonable to expect that this would not be apparent in a static  $^{65}\text{Cu}$  NMR spectrum if the differences in the Cu–S distances and bond angles are of this size. However, bond distances between Cu sites and the central S atom in this cubane structure have larger variations: all these are between  $2.67$  and  $2.71 \text{ \AA}$  (Table S1). Even more distinguishable differences in these structural parameters (and hence changes in a  $^{65}\text{Cu}$  NMR spectrum) could be expected when a complex has dithiophosphate ligands with longer, more bulky alkyl chains. As in the case of **III** with yet unknown crystal structure, the replacing of the  $\text{R} = -i\text{-C}_3\text{H}_7$  with  $\text{R} = -i\text{-C}_4\text{H}_9$  would be expected to indirectly distort the copper core and hence the Cu–S bond distances and bond angles. It is known that the larger the ligand, the lower the symmetry of the compounds is expected (*R-3* for  $\text{Cu}_8[\text{S}_2\text{P}(\text{OC}_2\text{H}_5)_2]_6(\text{S})$  [7], *C<sub>2/c</sub>* for  $\text{Cu}_8[\text{S}_2\text{P}(\text{O}-i\text{-C}_3\text{H}_7)_2]_6(\text{S})$  [5]). It is also expected that the systems with bulky “iso”-ligands would experience that trend more than the normal analogs. The static solid-state  $^{65}\text{Cu}$  NMR spectrum of **III** can therefore be considered as an example where the compound is most probably a mixture of  $\text{CuS}_3$  and  $\text{CuS}_3 \cdots \text{S}$  chemical environments. The copper core is distorted in such a way that half of the Cu-atoms are closer to the  $\text{S}_{\text{center}}$  and have higher-symmetry chemical environments of the tetrahedral  $\text{CuS}_3 \cdots \text{S}$  arrangement (the Cu-sites with smaller quadrupolar coupling constant ( $C_Q = 18.8$  MHz)). The other half of the copper atoms (the Cu-sites with bigger quadrupolar coupling constants ( $C_Q = 46.0$  MHz)) have the lower (planar) symmetry environments ( $\text{CuS}_3$ ), being considerably further away from the  $\text{S}_{\text{center}}$  and display a quadrupolar lineshape that is consistent with those of **I** and **II** where only the  $\text{CuS}_3$  environments are present.

In conclusion, to the best of our knowledge, we present here one of the first solid-state  $^{65}\text{Cu}$  NMR spectra of polycrystalline Cu(I) dialkyldithiophosphate compounds. The data, complemented with  $^{31}\text{P}$  MAS spectral data, can be used to probe the nuclearity of such Cu(I) systems and elucidate the structure of other polycrystalline copper(I) dithiophosphate systems. Work focusing on the NMR

characterization of similar cubane systems ( $\text{R} = -i\text{-C}_3\text{H}_7$  and  $-i\text{-C}_5\text{H}_{11}$ ) and the role of the embranchment of the hydrocarbon chain is in progress and will be published elsewhere. We also anticipate that these Cu(I) molecular systems can be used as models for future  $^{65}\text{Cu}$  NMR studies on small Cu(I)-metalloproteins in high magnetic fields.

### 3. Experimental details

#### 3.1. Synthesis of the clusters

##### 3.1.1. **I**: $\text{Cu}_4[\text{S}_2\text{P}(\text{O}-i\text{-C}_3\text{H}_7)_2]_4$

The complex was synthesized following a previously reported procedure [4] and recrystallized in  $\text{CH}_2\text{Cl}_2$  (65% yield).

##### 3.1.2. **II**: $\text{Cu}_6[\text{S}_2\text{P}(\text{OC}_2\text{H}_5)_2]_6$

The complex was obtained following the procedure by Liu et al. [5] in a  $\text{CH}_2\text{Cl}_2$ – $\text{H}_2\text{O}$  mixed solvent (60% yield). The obtained XRD spectra were compared to the calculated spectra of the compounds obtained with the *CrystalDiffract* calculation program (see Appendix A).

##### 3.1.3. **III**: $\text{Cu}_8[\text{S}_2\text{P}(\text{O}-i\text{-C}_4\text{H}_9)_2]_6(\text{S})$

The complex was prepared by reaction of CuCl (1 mmol) with  $\text{K}[\text{S}_2\text{P}(\text{O}-i\text{-C}_4\text{H}_9)_2]$  (1 mmol) in *N,N'*-dimethylformamide (DMF) in analogy to the method reported by Matsumoto et al. (45% yield) [7]. The FAB-mass of a freshly prepared sample shows a *m/e* of 1990 for the S-centered cluster,  $\text{Cu}_8[\text{S}_2\text{P}(\text{O}-i\text{-C}_4\text{H}_9)_2]_6 \text{SH}^+$ , and a strong peak at 977 consistent with the formation of a  $\text{Cu}_4[\text{S}_2\text{P}(\text{O}-i\text{-C}_4\text{H}_9)_2]_3$ -fragment. S/P elemental ratio for  $\text{C}_{48}\text{H}_{108}\text{Cu}_8\text{O}_{12}\text{P}_6\text{S}_{13}$  ( $M = 1988.361$ ): calculated  $-2.24$ , analytically obtained  $-2.23$ .

#### 3.2. NMR experimental conditions

All NMR experiments were performed at ambient temperature (298 K).

$^{31}\text{P}$  CP/MAS NMR. Solid-state  $^{31}\text{P}$  magic-angle-spinning (MAS) NMR spectra were recorded at  $145.73$  MHz on a Varian/Chemagnetics CMX Infinity 360 ( $B_0 = 8.46$  T) spectrometer with cross-polarization (CP) from the protons and with proton decoupling [14]. The CP mixing time was 3 ms. The proton  $\pi/2$  pulse duration was  $5 \mu\text{s}$  and 32 signal transients with a 3 s relaxation delay were accumulated. Polycrystalline samples (about 100 mg) were packed in standard zirconium (IV) oxide ( $\text{ZrO}_2$ ) 4 mm rotors. For reliable simulations of the chemical shift anisotropy parameters,  $^{31}\text{P}$  NMR spectra were obtained at three different spinning frequencies (3–5 kHz). All spectra were externally referenced to  $85.5\%$   $\text{H}_3\text{PO}_4$  [15].

Static  $^{65}\text{Cu}$  NMR. Solid-state  $^{65}\text{Cu}$  NMR spectra were recorded at  $170.39$  MHz on a Varian/Chemagnetics CMX Infinity 600 spectrometer equipped with a widebore 14.1 T magnet. The static spectra were collected using a Bruker 5 mm static probe. In all cases, a spin-echo sequence was applied ( $1.1 \mu\text{s} - \tau - 1.1 \mu\text{s}$  where  $\tau = 15 \mu\text{s}$ ).

The spectra were obtained with a pulse delay of 40 ms and 30,000–50,000 signal transients were accumulated. NMR data were processed in two different ways: (i) the whole echo was Fourier transformed (FT); (ii) FID data were left-shifted to the echo maximum prior to FT (half echo). Because of the width of the powder lineshapes, excitation at a single frequency was insufficient to excite the whole spectrum; the spectra were therefore acquired by stepping the frequency by 100 kHz, retuning the probe, acquiring a new set of data and finally adding all the sub-spectra together. All spectra were externally referenced to a secondary standard of powdered CuCl [16].

### 3.2.1. Simulations of $^{65}\text{Cu}$ NMR spectra

The second-order-like quadrupolar lineshapes for the central transition of copper-65, with a significant CSA contribution, were fitted using the *DMFit* program [17] and the NMR interaction parameters for the copper(I) dialkyldithiophosphate complexes were obtained from these simulations (Table 2). The errors in Table 2 were estimated by changing a parameter value when all of the other parameter values were kept constant. In addition to these fits, the  $^{65}\text{Cu}$  NMR spectra were simulated using the SIMPSON simulation program [18] and the NMR parameters obtained by *DMFit* were confirmed independently.

### 3.2.2. Simulations of $^{31}\text{P}$ CSA

Simulations of the  $^{31}\text{P}$  chemical shift anisotropies were performed in a Mathematica-based program developed by Levitt and co-workers [19].

## Acknowledgments

The work was financed by ARC at Luleå University of Technology and the Marie Curie Industry Host Fellowship HPMT-CT-2001-00335-02. The Varian/Chemagnetics CMX 360 spectrometer was purchased with a grant from the Swedish Council for Planning and Coordination of Research (FRN) and upgraded further with a grant from the Foundation to the memory of J.C. and Seth M. Kempe. Authors also acknowledge CHEMINOVA AGRO A/S for the dialkyldithiophosphate chemicals. We are grateful to Marshall Hughes, Organic Mass Spectroscopy Facility in the CSL at University of Tasmania, for the FAB-mass measurements of compound III. We thank Dr. Andy Howes and Professor Mark E. Smith, University of Warwick, UK, for discussions.

## Appendix A. Supplementary data

Supplementary data (the XRD powder patterns of the corresponding compounds, the detailed simulation of the  $^{65}\text{Cu}$  NMR spectrum of III, and the  $^{65}\text{Cu}$  NMR response of the systems at the direct excitation mode) associated with this article can be found, in the online version, at doi:10.1016/j.jmr.2005.10.013.

## References

- [1] F. Sabin, C.K. Ryu, P.C. Ford, Photophysical properties of hexanuclear copper(I) and silver(I) clusters, *Inorg. Chem.* 31 (1992) 1941–1945.
- [2] (a) I.G. Dance, The structural chemistry of metal thiolate complexes, *Polyhedron* 5 (1986) 1037–1104; (b) G. Henkel, B. Krebs, Transition-metal thiolates: from molecular fragments of sulfidic solids to models for active centers in biomolecules, *Angew. Chem. Int. Ed. Engl.* 30 (1991) 769–788.
- [3] A.N. Buckley, S.W. Goh, R.N. Lamb, R. Woods, Interaction of thiol collectors with pre-oxidised sulfide minerals, *Int. J. Miner. Process.* 72 (2003) 163–174.
- [4] W. Lawton, J. Rohrbach, G.T. Kokotailo, Crystal and molecular structure of the tetranuclear metal cluster complex copper(I) *O,O'*-diisopropylphosphorodithioate,  $\text{Cu}_4[(\text{iso-PrO})_2\text{PS}_2]_4$ , *Inorg. Chem.* 11 (1972) 612–618.
- [5] C.W. Liu, T. Stubbs, R.J. Staples, J.P. Fackler Jr., Syntheses and structural characterizations of two new Cu–S clusters of dialkyldithiophosphates: a sulfide-centered  $\text{Cu}_8^1$  cube,  $\{\text{Cu}_8[\text{S}_2\text{P}(\text{O}i\text{Pr})_2]_6(\mu_8\text{-S})\}$ , and a distorted octahedral  $\{\text{Cu}_6[\text{S}_2\text{P}(\text{OEt})_2]_6 \cdot 2\text{H}_2\text{O}\}$  cluster, *J. Am. Chem. Soc.* 117 (1995) 9778–9779.
- [6] Z.X. Huang, S.F. Lu, J.Q. Huang, D.M. Wu, J.L. Huang, Synthesis and structure of  $\text{Cu}_8\text{S}[\text{S}_2\text{P}(\text{OC}_2\text{H}_5)_2]_6$ , *Jiegou Huaxue (J. Struct. Chem.)* 10 (1991) 213–217.
- [7] K. Matsumoto, R. Tanaka, R. Shimomura, Y. Nakao, Synthesis and X-ray structures of octanuclear silver(I) cluster  $[\text{Ag}_8(\mu_6\text{-S})\{\text{S}_2\text{P}(\text{OC}_2\text{H}_5)_2\}_6]$  and its copper(I) analogue  $[\text{Cu}_8(\mu_8\text{-S})\{\text{S}_2\text{P}(\text{OC}_2\text{H}_5)_2\}_6]$ , *Inorg. Chim. Acta* 304 (2000) 293–301.
- [8] I. Haiduc, D.B. Sowerby, S.-F. Lu, Stereochemical aspects of phosphor-1,1-dithiolato metal complexes (dithiophosphates, dithiophosphinates): coordination patterns, molecular structures and supramolecular associations—I, *Polyhedron* 14 (1995) 3389–3472.
- [9] A.-C. Larsson, A.V. Ivanov, W. Forsling, O.N. Antzutkin, A.E. Abraham, A.C. de Dios, Correlations between  $^{31}\text{P}$  chemical shift anisotropy and molecular structure in polycrystalline *O,O'*-dialkyldithiophosphate Zinc(II) and Nickel(II) complexes:  $^{31}\text{P}$  CP/MAS NMR and ab initio quantum mechanical calculation studies, *J. Am. Chem. Soc.* 127 (2005) 2218–2230.
- [10] T.J. Bastow, M.E. Smith,  $^{91}\text{Zr}$  NMR characterization of phase in transformation toughened zirconia, *Solid State Nucl. Magn. Reson.* 1 (1992) 165–174.
- [11] T.J. Bastow, M.E. Smith,  $^{139}\text{La}$  Nuclear magnetic resonance characterisation of  $\text{La}_2\text{O}_3$  and  $\text{La}_{1-x}\text{Sr}_x\text{MO}_3$  where  $\text{M} = \text{Cr}, \text{Mn}$  or  $\text{Co}$ , *Solid State Nucl. Magn. Reson.* 3 (1994) 17–22.
- [12] S. Schramm, E. Oldfield, High-resolution oxygen-17 NMR of solids, *J. Am. Chem. Soc.* 106 (1984) 2502–2506.
- [13] D. Rusanova, W. Forsling, O.N. Antzutkin, K.J. Pike, R. Dupree, Formation of  $\{\text{Cu}_6[\text{S}_2\text{P}(\text{OC}_2\text{H}_5)_2]_6\}$  on  $\text{Cu}_2\text{S}$  surfaces from aqueous solutions of the  $\text{KS}_2\text{P}(\text{OC}_2\text{H}_5)_2$  collector: scanning electron microscopy and solid-state  $^{31}\text{P}$  cross-polarization/magic angle spinning and static  $^{65}\text{Cu}$  NMR studies, *Langmuir* 21 (2005) 4420–4424.
- [14] A. Pines, M.G. Gibby, J.S. Waugh, Proton-enhanced nuclear induction spectroscopy. A method for high resolution NMR of dilute spins in solids, *J. Chem. Phys.* 56 (1972) 1776–1777.
- [15] K. Karaghiosoff, Phosphorus-31 NMR, in: D.M. Grant, R.K. Harris (Eds.), *Encyclopedia of Nuclear Magnetic Resonance*, vol. 6, Wiley, New York, 1996, pp. 3612–3618.
- [16] K.J.D. Mackenzie, M.E. Smith, K.J.E. Dunn, *Multinuclear Solid-state Nuclear Magnetic Resonance of Inorganic Materials*, Pergamon Press, New York, 2002.
- [17] D. Massiot, F. Fayon, M. Capron, I. King, S. Le Calvé, B. Alonso, J.-O. Durand, B. Bujoli, Z. Gan, G. Hoatson, Modelling one and two-dimensional solid-state NMR spectra, *Magn. Reson. Chem.* 40 (2002) 70–76.

- [18] M. Bak, J.T. Rasmussen, N.C. Nielsen, SIMPSON: a general simulation program for solid-state NMR spectroscopy, *J. Magn. Reson.* 147 (2000) 296–330.
- [19] O.N. Antzutkin, Y.K. Lee, M.H. Levitt,  $^{13}\text{C}$  and  $^{15}\text{N}$ -chemical shift anisotropy of ampicillin and penicillin-V studied by 2D-PASS and CP/MAS NMR, *J. Magn. Reson.* 135 (1998) 2218–2230.